



Prediction of the creeping of AFC based on fuzzy reasoning and Bi-LSTM fusion iteration

Suhua Li^{1,2} · Jiacheng Xie^{1,2} · Xuewen Wang^{1,2} · Fuxiang Ge^{1,2}

Accepted: 18 April 2024
© The Author(s) 2024

Abstract

The creeping of Armoured Face Conveyor (AFC) is an engineering problem that needs to be avoided in coal mining production process. In this paper, a method for predicting the creeping accident of AFC based on fuzzy reasoning and Bi-directional Long Short-Term Memory (Bi-LSTM) fusion iteration is put forward. Firstly, through the force analysis of the AFC and the fuzzy correlation analysis method in the actual operation process, the reasons for the creeping of AFC are analyzed; Secondly, according to the propulsion characteristics of the AFC in the time sequence development, the method of the AFC running track based on Bi-LSTM neural network is proposed; Then, on the basis of the virtual transformation of the prediction results, a judgment mechanism for the extent of the creeping of the AFC based on fuzzy evidence reasoning based on fuzzy comprehensive evaluation method and Dempster-Shafer evidence theory (D-S evidence theory) is established; Finally, the analysis on the creeping of 9711 full-mechanized mining face in Kaiyuan Mine under virtual environment after 6 cycles of continuous advancement shows that the extent of creeping of AFC is relatively high and coal mining accidents are likely to occur.

Keywords AFC · Creep · Digital Twin · Bi-LSTM · Fuzzy Comprehensive Evaluation · D-S evidence theory

With the rapid development of production and manufacturing towards intelligence (Kang et al. 2016), the fast-paced and less humanized production mode brings high efficiency, low cost and high benefit. At the same time, with the potential impact of uncertain factors such as production environment, climate and personnel operation, some accidents will bring irreversible engineering accidents (Qiang 2020), which will bring huge losses to human, material and financial resources. The development of digital twin technology, artificial intelligence technology and human-computer interaction technology provides technical support for the analysis of engineering problems such as analyzing the causes of

✉ Xuewen Wang
wangxuewen@tyut.edu.cn

¹ College of Mechanical and Vehicle Engineering, Key Laboratory of Fully Mechanized Coal Mining Equipment, Taiyuan University of Technology, Shanxi 030024, China

² Taiyuan University of Technology, No.216 Mailbox HuYu Campus, No.18, XinKuangYuan Road, TaiYuan, ShanXi Province, People's Republic of China

engineering accidents, predicting the development trend of production process and judging the development degree of engineering accidents (Le and Ahn 2011). If based on the above technology, a pertinent analysis platform for engineering accidents can be established, a prediction mechanism facing the development trend of production process or accident and an accident decision-making and analysis mechanism can be established, potential problems in current production process or the development degree of engineering accidents can be found, and corresponding countermeasures can be provided, which can achieve the purpose of providing timely and effective solutions to engineering problems and reduce the impact of accidents.

The coal mining industry usually belongs to the typical deep space operation production, the production environment is bad, the geological environment is complex, and there are many uncertain factors interfering with the production process. With the advancement of intelligent coal mining (Huang et al. 2020), the requirements for unmanned mining have become higher, and a safer and more efficient mining mode is being pursued (Wang and Huang 2017). However, in the mining process, under the combined action of coal seam fluctuation and equipment interaction, it is easy to cause some accidents that are difficult to avoid. The creeping of Armoured Face Conveyor (AFC) is one of the common and typical engineering problems in the process of coal mining. The small movement of the line pan of the AFC will affect the straightness of the whole fully mechanized mining face. When the movement is serious, it will even cause the equipment to accumulate (Peng et al. 2019), resulting in major mining accidents. This paper selects the engineering problem of the creeping of AFC as an example to build the general prediction framework of accident, and provides research framework and key technical support for other engineering problems.

Relevant technical teams and scholars (CSIRO 2021; Zhang et al. 2018; Michael and Hainsworth 2005; Song and Wang 2014; Niu 2015) have studied the mechanism and control of the up-slip of AFC, but there are still the following deficiencies in the research of creeping on fully-mechanized mining face. Firstly, when analyzing the cause mechanism and establishing the mechanical model, the analysis idea is mostly the single factor analysis method, which ignores the correlation between the factors, i.e., the influence of the chain effect brought by the joint action of the factors on the equipment position state. Therefore, in the process of research, it is more one-sided to analyze only the single factor for the creeping of the AFC. Secondly, the analysis of the mechanism of the creeping of AFC is carried out under ideal coal seam conditions, resulting in a certain gap between the research environment and the actual environment in the whole analysis process. When analyzing the mechanism of equipment creep in the whole mining environment, it only judges whether the equipment moves based on the visual perception of miners, and there is no specific measurement standard for the degree of creeping. Thirdly, it is found that after the adjustment of the conveyor, the creeping of the equipment has been reduced, i.e., the technical control of the scraper has been improved, which has a certain impact on the decline of the mining technology.

With the development of digital twin technology, the establishment of digital twin of physical environment and the simulation and pre-experiment in virtual environment can provide conclusions and scheme support for the research in physical environment (Xie et al. 2022; Guo et al. 2019). As a virtual simulation engine that supports multi-dimensional and interactive graphical development environment, Unity3D can realize the visualization of complex working environment and establish the digital twin of physical environment (Cai et al. 2023). The existing research (Ge et al. 2020; Shen et al. 2021) shows that the virtual simulation and research of coal mine underground related work in Unity3D has great advantages, and can provide visual ideas and research schemes for solving the

problems such as the creeping of fully mechanized mining face. Therefore, in view of the problems and deficiencies existing in the current research, a visual analysis platform for the creeping of the AFC can be created in Unity3D. During the simulation process, the reconstruction and extrapolation of the motion trajectory of the digital twin model is one of the keys to support the subsequent research, which requires further prediction of the periodic properties of the trajectory extracted in space and time to support the relevant analysis of future working conditions. The application of commonly used neural networks in performing trajectory prediction is shown in Table 1.

From Table 1, it can be seen that compared to other networks, the Bi-LSTM neural network can better predict the next state by simultaneously predicting the forward and backward directions during time series prediction. Bi-LSTM neural network has a good application in the prediction and diagnosis of power supply and demand prediction (Özer et al. 2021), load prediction (Yeming et al. 2022) fault diagnosis (Tong et al. 2021) and other events related to timing processing (Özer et al. 2021). The characteristic of such events is that it is necessary to predict and judge the future data according to the historical data and the characteristics of the data is periodic. In the mining process, when there are no folds, faults and other complex geological structures of the coal seam, the overall fluctuation of the coal seam floor is small, so that the floor changes gently in the continuous space–time advance, (Guo et al. 2019), which makes there are small differences between the laying trajectories of the AFC. The fixity of the coal mining process, coupled with the influence of the coal cutting mode of memory cutting, makes the AFC trajectories also have periodic changes in the process of advancing with the reciprocating cutting operation of the shearer

Table 1 Common neural networks for trajectory prediction

Type	Application	Characteristics
Generative Adversarial Nets (GAN)	trajectory of aircraft (Xiping et al. 2022)	The ability of generation and generalization is strong, but the training is unstable
Convolutional Neural Networks (CNN)	Pedestrian trajectory (Simone et al. 2022)	Feature extraction ability and generalization ability are strong, but there is no memory function
Recurrent Neural Network (RNN)	Obstacle vehicle trajectory (Min et al. 2019)	Good at processing time series data, but not suitable for long-distance dependence
Gated Recurrent Unit (GRU)	Pipe jacking machine trajectory (Feng et al. 2023)	Better at capturing long-term dependencies, but not for complex sequential dependencies
Long Short Term Memory (LSTM)	Pedestrian trajectories (Quan et al. 2021)	Can capture dependencies over long-term, but with only historical information as input
Bi-directional Long Short-Term Memory (Bi-LSTM)	Tire trajectory (Shenguang et al. 2023)	Introducing reverse information from the time dimension to better capture the characteristics of data, but it is easy to over fit

(CSIRO 2021). Therefore, Bi-LSTM neural network algorithm can also be applied to the prediction process of the position coordinates of the AFC. When the predicted position trajectory of the AFC is obtained, there is a positioning benchmark for the position of relevant equipment in the virtual environment in the future, but whether the position state of the equipment is normal or not is still unknown. Therefore, it is necessary to establish a judgment mechanism for this uncertain event of abnormal position state of the equipment. According to the prediction information, the accidents or accident grades that may be caused in the future mining are evaluated, so as to provide ideas for the subsequent mining process adjustment. Dempster-Shafer evidence theory (D-S evidence theory) is a complete theory for dealing with uncertain events (Dempster 1967, 1968). It shows great flexibility in distinguishing unknown events, uncertain events (Wang et al. 2022) and event evaluation (Jie et al. 2021). The treatment of fuzzy events based on D-S evidence theory is a relatively reliable decision-making method. Therefore, this paper adopts D-S evidence theory to make a decision on the degree of the creeping of AFC.

Based on the above contents, this paper carries out a visual comprehensive analysis on the creeping mechanism of AFC from the perspective of virtual-real mapping based on the digital twin theory. Bi-LSTM neural network model in virtual running environment was built to forecast position coordinate track of AFC in continuous propulsion. On the premise that the predicted results can be converted into information of virtually drive the AFC, a judgment mechanism of creeping degree of AFC based on fuzzy D-S evidence theory in virtual environment is established to judge the creeping degree of AFC, and finally to provide guidance for the change of mining technology scheme of the next knife. The above contents are integrated and a virtual simulation system for visual analysis of the creeping of AFC is established.

1 Overall framework

Aiming at the problem of the creeping of AFC during coal mining, from the point of view of accident occurrence mechanism and production and operation data, this paper integrates digital twin technology with predictive analysis technology, and establishes a research framework to solve such engineering problems based on multi-disciplinary analysis theory. The overall framework is shown in Fig. 1.

Taking Unity3D as the main research and analysis platform, and based on the analysis of the causes and mechanism of the creeping of the AFC, this paper establishes the prediction model of propulsion trajectory and the judgment model of the creeping degree, and realizes the prediction of the occurrence and development degree of the engineering problem. The process is as follows:

- (1) Analysis on influencing factors of the creeping of AFC. According to the reasons for the creeping of the AFC in the actual propulsion process, the corresponding influencing factors are determined in the virtual environment based on the digital twin theory, and the influencing factors of the AFC are analyzed based on the fuzzy grey correlation analysis.
- (2) Trajectory prediction of AFC based on Bi-LSTM neural network. The configuration parameters of the virtual simulation environment are determined on the basis of content (1). According to the similarity and periodicity of the trajectory during propulsion,

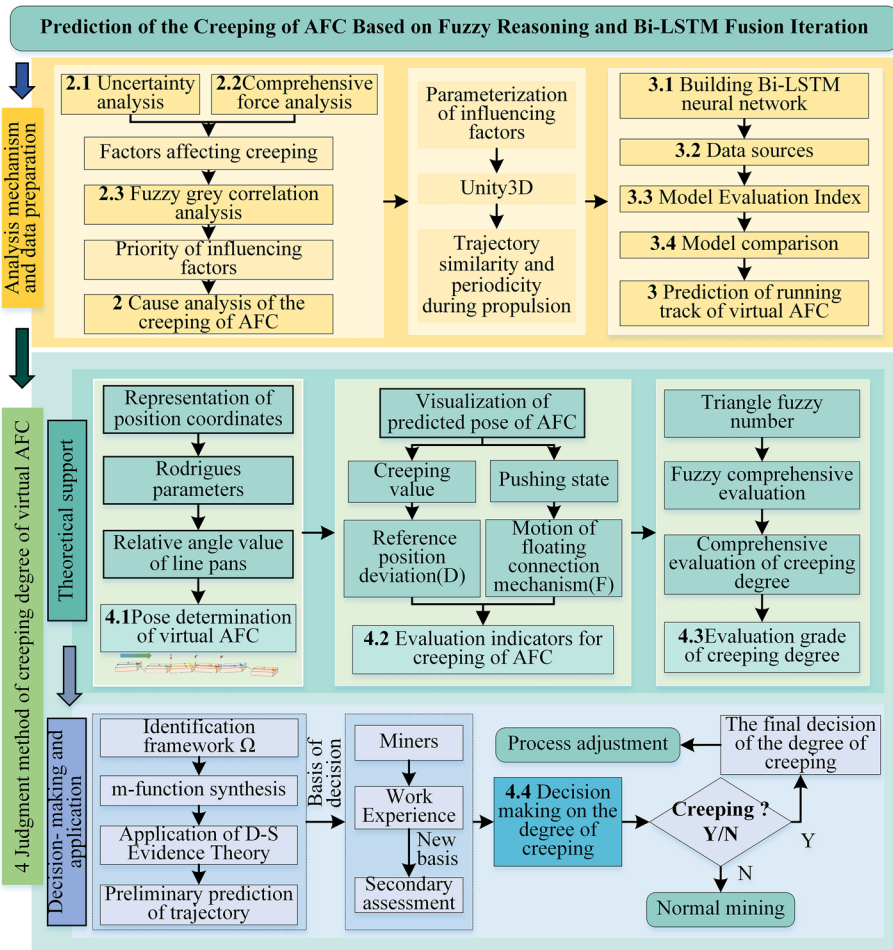


Fig. 1 Method flow chart of the paper

Bi-LSTM neural network is selected to predict the trajectory of AFC in this paper. According to the characteristics of coordinate points in the propulsion process of AFC in virtual environment, the prediction model of AFC running trajectory is established. In view of the characteristics of virtual equipment position coordinates, the data set is established. Compared with the traditional LSTM neural network, it further proves the reliability of this model.

- (3) The judgment mechanism of creeping degree of AFC based on fuzzy evidence reasoning theory. The prediction results are transformed, and the evaluation degree grade of the creeping of AFC is established based on fuzzy comprehensive evaluation method. Then, the evaluation method of creeping degree of AFC based on D-S evidence theory is proposed to determine the development degree of current accident and provide corresponding countermeasures.

2 Cause analysis of the creeping of AFC based on digital twin and fuzzy grey correlation analysis

When predicting the degree of creeping on the AFC, it is necessary to analyze the root cause of this engineering problem. The shearer, hydraulic support, and AFC are the core equipment of the fully mechanized mining face (Niu 2015). During the production process, the operating status of the shearer and hydraulic support will have a certain impact on the operation of the AFC.

2.1 Uncertainty performance in determining the degree of creeping of AFC

- (1) **The uncertainty of 3D modeling of coal seam.** In the process of judging the creeping of the AFC, the fineness of the 3D modeling of the coal seam environment is one of the key factors. In the process of constructing a coal seam 3D model, it is susceptible to various factors such as the complexity of coal seam structure, inaccuracy or inconsistency of modeling data, and subjectivity of modeling personnel, which inevitably leads to a certain degree of uncertainty in the established 3D model of coal seam. These uncertainties often cause a certain degree of deviation in the vertical resolution of the constructed coal seam 3D model, and limiting its further application level.
- (2) **The uncertainty of the impact of auxiliary mining processes.** During the advancement of the fully mechanized mining face, dust reduction will be carried out by sprinkling water as the mining progresses, which reduces the frictional force between the equipment and the coal seam floor during advancement. Coupled with the uncertainty of the coal seam, it may promote the occurrence of creeping phenomenon. In addition, during the comprehensive mining construction, there may be a phenomenon of bulging of the bottom plate, which causes the AFC to curl up and cause the creeping during propulsion.
- (3) **The uncertainty of straightness of AFC.** However, due to the spatial motion characteristics of the hydraulic support during movement, the displacement of the line pan generated during movement is minimal, and gradually accumulates with advancement, resulting in the randomness of the straightness of the AFC (Li et al. 2022). The circular motion of the line pan during movement will generate lateral thrust on adjacent equipment, driving the occurrence of creeping.

2.2 Comprehensive analysis of force on AFC

2.2.1 Force analysis of the AFC

The force analysis of the AFC when it creeps mainly focuses on the sources of influence from the environment and equipment (Fig. 2).

- (1) **Environmental impact of mining.** When the inclination angle of the coal seam is too large, the AFC may creep under the influence of gravity such as the shearer, coal blocks (Holm 2014), and its own gravity (refers to G). Due to the frequent watering and dust spraying on the working face, the friction coefficient is further reduced, changing the magnitude of the friction force F_f , causing the AFC to creep.

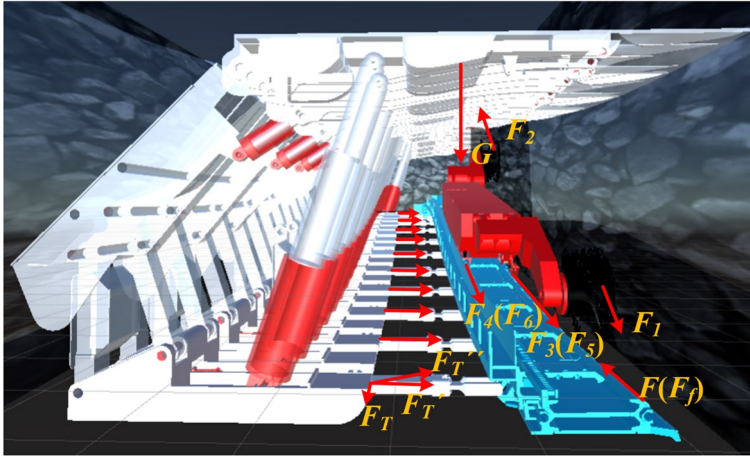


Fig. 2 Force analysis of the AFC

- (2) **The cutting force of the shearer is affected.** The shearer uses a scraper conveyor as a platform and anchor point (Hu 2016), which will apply opposite forces (F_4, F_6) on the AFC; In addition, the resistance (F_1, F_2) generated by the shearer when cutting the coal wall, as well as the running resistance (F_3, F_5) generated between the sliding shoe and the AFC, which may cause the scraper conveyor to creep.
- (3) **The influence of the pushing posture of the AFC.** During the propulsion process of the AFC, it will go through two stages: serpentine and straightening, and will be subject to resistance from the straight section during operation and resistance from the curved section during operation. These two resistances constitute the main part of the operating resistance (F) of the AFC, which will to some extent affect the creep;
- (4) **The influence of hydraulic support pushing force.** When the hydraulic support group and the AFC are in a misaligned state, the force will be distributed along the coal seam inclination (refers to F_7), which will also have an impact on the creeping of the AFC.

2.2.2 Comprehensive analysis of force

According to the above analysis, the creeping force of the AFC can be analyzed from the force promoting or hindering the creeping of the AFC.

In any case, the gravity of the equipment and coal blocks has the force F' to promote the downslide of the AFC. The resistance F of the AFC during propulsion and the friction F_f of the AFC during propulsion will prevent the downslide of the AFC.

The force generated by the shearer traction on the AFC is opposite to the traction direction. When the shearer is upward cutting, the force F_3', F_4', F_5', F_6' of the shearer on the AFC will promote the AFC to downslide, and vice versa.

The force of the hydraulic support on the AFC is related to the swing direction of the push rod. When pushing the AFC, when the push rod is inclined downward as a whole, it will promote the AFC to downslide.

In conclusion, the comprehensive effects of various forces on the creeping of AFC are shown in Table 2.

When the shearer goes up to cut coal, the resultant force to promote the AFC to downslide is F_d , the total force preventing the AFC from downslide is F_{sd} .

2.3 Factor analysis of creeping mechanism in virtual environment based on fuzzy grey correlation analysis

Corresponding to Sect. 2.2, the factors influencing the creeping of AFC in virtual environment mainly include inclination along the direction of coal seam, friction coefficient between the equipment and the floor, and attributes of related forces, the coupling effect between these factors has significant uncertainty, fuzziness, and grayness. In actual production, different degrees of creeping of the AFC correspond to different response measures. However, the degree of creeping is a vague concept, and the analysis of this degree in the mining process is often judged based on the production experience of coal miners. Once a misjudgment occurs, it may lead to irreversible consequences. Therefore, this paper aims at the fuzzy variable of the degree of creeping of the AFC, combines the fuzzy theory with the grey correlation analysis method, and objectively carries out the correlation analysis on the influencing factors of creeping of the AFC. In this paper, the AFC is regarded as a rigid structure (Xu 1999; Verma 2013; Wang et al. 2020), the force of the hydraulic support push rod on the AFC can be regarded as the effect of external force, and the connection between the hydraulic support push rod and the AFC is realized by kinematics method.

On the basis of realizing the virtual connection between the hydraulic support and the AFC (Li et al. 2021), the reference position variation of the creeping of the AFC is selected as the reference sequence $Y\{k\}$, which is used as the data sequence to study the characteristics of behavior of the AFC. The data variation law of each group of plans can be regarded as the actual change of creeping, and the relation is shown in Eq. (1).

$$Y\{k\} = [Y\{1\}Y\{2\}Y\{3\} \dots Y\{n\}] \tag{1}$$

The comparison sequence is friction coefficient $X_1\{k\}$, coal seam inclination $X_2\{k\}$, the force of shearer $X_3\{k\}$, Angular Drag value $X_4\{k\}$, Drag value $X_5\{k\}$, which reflects the data sequence of influencing factors on the change of reference position of the creeping of the AFC. It is assumed that there are n experimental plans and the corresponding comparative sequence matrix is shown in Eq. (2).

$$X_k = \begin{bmatrix} X_1\{k\} \\ X_2\{k\} \\ X_3\{k\} \\ X_4\{k\} \\ X_5\{k\} \end{bmatrix} = \begin{bmatrix} X_1\{1\} & X_1\{2\} & X_1\{k3\} & \dots & X_1\{n\} \\ X_2\{1\} & X_2\{2\} & X_2\{3\} & \dots & X_2\{n\} \\ X_3\{1\} & X_3\{2\} & X_3\{3\} & \dots & X_3\{n\} \\ X_4\{1\} & X_4\{2\} & X_4\{3\} & \dots & X_4\{n\} \\ X_5\{1\} & X_5\{2\} & X_5\{3\} & \dots & X_5\{n\} \end{bmatrix} \tag{2}$$

Due to the different dimensions of data in each factor, it is impossible to directly compare and analyze the values. Therefore, in order to ensure the reliability of the analysis results, dimensionless processing of variables is required, as shown in Eq. (3).

$$X_i\{k\} = \frac{X_m\{k\}}{\frac{1}{n} \sum_{i=1}^k X_i\{k\}}, k = 1, 2 \dots n, m = 1, 2 \dots 5 \tag{3}$$

Table 2 Comprehensive analysis of creeping forces of AFC

Direction of shearer cutting	Oscillation of push rod	F_d	F_{sd}	Creeping direction
Upward cutting	Overall inclined downward	$F_d = F_l + F_3' + F_4' + F_5' + F_6' + F_T$	$F_{sd} = F + F_f$	Downslide: $F_d > F_{sd}$
	Overall inclined upward	$F_d = F_l + F_3' + F_4' + F_5' + F_6'$	$F_{sd} = F + F_f + F_T$	Upward Upward $F_d < F_{sd}$
Downward cutting	Overall inclined downward	$F_d = F_l + F_T$	$F_{sd} = F + F_f + F_3' + F_4' + F_5' + F_6'$	
	Overall inclined upward	$F_d = F_l$	$F_{sd} = F + F_3' + F_4' + F_5' + F_6' + F_T$	

To describe the degree of belonging to different evaluation levels, the included cosine method is used to calculate the fuzzy membership, which is not affected by the linear proportional relationship of data. The similarity between reference and comparison series can be determined by the included cosine value between parameters, as shown in Eq. (4).

$$r_i = \frac{\sum_{i=1}^m Y\{k\}X_i\{k\}}{\sqrt{\sum_{k=1}^n Y\{k\}^2} \sqrt{\sum_{k=1}^n X_m\{k\}^2}}, m = 1 \dots 5 \tag{4}$$

Through the design of different experimental schemes, the environment setting of each influencing factor in the simulation system is carried out to promote the virtual AFC, and the position change parameter value $Y\{k\}$ of the AFC under different experimental schemes is obtained. Calculating grey correlation coefficient between the comparison sequence and the reference sequence $\xi_i(k)$. This coefficient shown in Eq. (5) reflects the degree of correlation between the reference sequence and the comparison sequence.

$$\xi_i(k) = \frac{\min_i \min_k |Y\{k\} - X_i\{k\}| + \rho \max_i \max_k |Y\{k\} - X_i\{k\}|}{|Y\{k\} - X_i\{k\}| + \rho \max_i \max_k |Y\{k\} - X_i\{k\}|}, k = 1, 2 \dots 5, \tag{5}$$

where, ρ is the resolution coefficient, $\rho \in [0, 1]$. According to the value principle of ρ (Deng 1988), when $\rho \leq 0.5$, it is easier to observe the changes in resolution of $\xi_i(k)$ on $X_i\{k\}$ and $Y\{k\}$; However, in order to monitor the amount of creeping, the selected reference sequence $Y\{k\}$ has a relatively stable value, and ρ should be taken as the larger value, so $\rho=0.5$ is extracted in this paper.

As the values of multiple correlation coefficients are scattered, it is difficult to make overall comparison. The correlation degree $\xi_i(k)$ between each comparison sequence and reference sequence is averaged in different dimensions. The obtained r_i' values are regarded as grey correlation degree, as shown in Eq. (6).

$$r_i' = \frac{1}{n} \sum_{i=1}^k \xi_i(k), k = 1, 2, \dots, 5, n = 5 \tag{6}$$

When comprehensively comparing the influencing factors of the creeping of the AFC, the two evaluation indexes of $\xi_i(k)$ and r_i' are oriented to different mining stages. The former focuses on the impact on the creeping of the AFC when various influencing

factors change due to process switching during single-cutting propulsion; The latter focuses on the influence of various factors in the overall propulsion, starting from the perspective of the correlation between the cutting floors, and after comprehensively considering the impact of process switching and equipment movement on the degree of creeping. Therefore, both indicators are equally important for evaluating the degree of creeping during propulsion and independent, this paper adopts linear weighted synthesis method to merge, and obtain the comprehensive index value of influencing factors on the AFC propulsion, i.e. the fuzzy grey correlation degree is obtained. The expression is shown in Eq. (7).

$$R_i = \frac{1}{2} \left(\frac{\sum_{i=1}^m Y\{k\}X_i\{k\}}{\sqrt{\sum_{k=1}^n Y\{k\}^2} \sqrt{\sum_{k=1}^n X_m\{k\}^2}} + \frac{1}{n} \sum_{i=1}^k \xi_i(k) \right) \tag{7}$$

According to the above contents, the priority of each influencing factor in virtual environment to the impact degree of the creeping of AFC can be obtained. The propulsion environment of AFC can be configured according to the optimal scheme, and the obtained track information can be used as the data source for prediction analysis, so as to predicate the current running state of AFC.

3 Prediction of running track of virtual AFC based on Bi-LSTM neural network

Due to the workflow of the coal mining process and the memory of the cutting process of the shearer, the track obtained by the AFC during the driving process has certain similarity in the adjacent two knives, and shows certain periodicity with the fluctuation and cutting of the coal seam. Under the premise of realizing the visualization of virtual simulation environment and the optimization of environmental factors, the trajectory of the current AFC can be predicted according to the change law of the trajectory of the two adjacent AFC in the historical information in the time series.

3.1 Bi-LSTM neural network

LSTM is composed of input gate, forget gate, and output gate (Hochreiter and Schmidhuber 1997), which control the state of the cell and the state of the hidden layer, and delete or add information to it. The calculation model is shown in Eqs. (8) - (13).

$$f_t = \sigma(W_f, [h_{t-1}, x_t] + b_f) \tag{8}$$

$$i_t = \sigma(W_i, [h_{t-1}, x_t] + b_i) \tag{9}$$

$$\hat{c}_t = \tanh(W_c, [x_t, h_{t-1}] + b_c) \tag{10}$$

$$c_t = f_t * c_{t-1} + i_t * \hat{c}_t \tag{11}$$

$$o_t = \sigma(W_o, [h_{t-1}, x_t] + b_o) \tag{12}$$

$$h_t = o_t * \tanh(c_t) \tag{13}$$

where, f_t, i_t, o_t stands for Forgetting gate, Input gate and Output gate respectively; c_{t-1} represents the memory state of the cell at the previous time, c_t, \hat{c}_t represents the memory state of cell unit; h_{t-1} represents the output state of the cell unit at the previous time, h_t represents the output state of the cell unit at the current time; x_t represents the input state of the current cell unit; $W_f, W_i, W_o, b_f, b_i, b_o$ is an adjustable parameter matrix or vector.

However, the information in LSTM is one-way transmission, which only learns the influence of historical state on current state, without fully utilizing the dependency relationship between time series (Quan et al. 2021). Considering that the position of the AFC is more susceptible to the influence of the floor undulation and the equipment forces, as well as the long cutting cycle time sequence of the fully-mechanized mining face, Bi-LSTM is selected to establish the prediction model. As shown in Fig. 3, the independent Bi-LSTM neural network is used to extract the timing feature information from the historical running track of AFC, and the obtained feature information is spliced by feature fusion technology. The splicing information is input to the second layer Bi-LSTM network. The final output is the splicing of the results with two directions forecast.

Bi-LSTM processes the timing data independently through the forward layer and the backward layer. The forward layer can obtain the past data information of the input sequence, and the backward layer can obtain the future data information of the input sequence, and transmit the processing results to the output layer at the same time, which can make full use of the characteristics contained in the past and future data. At time t , the forward and backward output results of Bi-LSTM are shown in Eqs. (14)-(16).

$$\vec{h}_t = \overrightarrow{\text{LSTM}}(h_{t-1}, x_t, c_{t-1}) \tag{14}$$

$$\overleftarrow{h}_t = \overleftarrow{\text{LSTM}}(h_{t+1}, x_t, c_{t+1}) \tag{15}$$

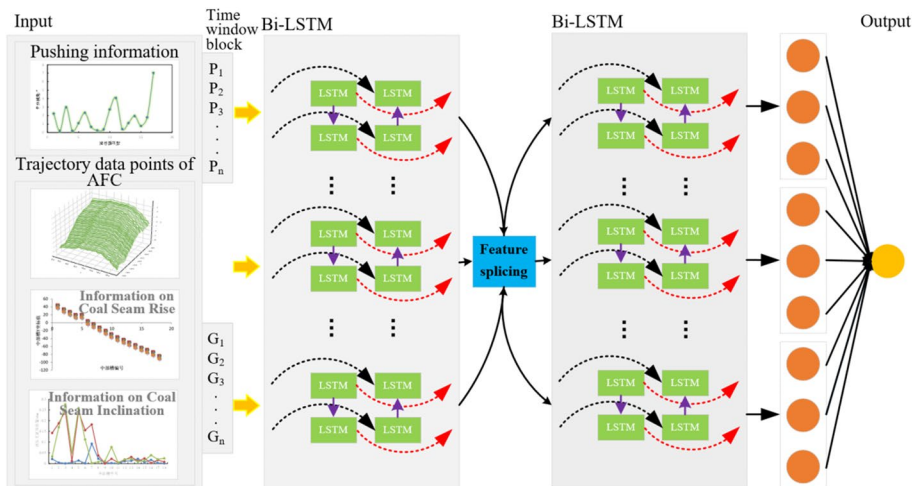


Fig. 3 Track prediction model of AFC based on Bi-LSTM neural network

$$H_t = \vec{h}_t + \overleftarrow{h}_t \quad (16)$$

where, H_t is the output value of the hidden layer, \vec{h}_t is the output value of the forward layer and \overleftarrow{h}_t is the output value of the backward layer.

The trajectory point characteristics of the AFC with t -th blade are represented as $x_t = (t, x_t^i, y_t^i, z_t^i, d^i, \varphi^i)$, (x_t^i, y_t^i, z_t^i) contains information on the undulations and dip angles of coal seam; The trajectory point of the AFC with $t+1$ blade is $y_{t+1} = (t, x_t^i, y_t^i, z_t^i)$; The mapping function between the output value and the input value is defined as $y_{t+1} = f(x_t, x_{t-1}, \dots, x_{t-T+2}, x_{t-T+1})$.

This model learns the correlation and temporal dependencies between data by stacking multiple Bi-LSTM networks, and predicts the trajectory of the AFC through a fully connected layer and a regression layer. The input information in the model is $X = (x_{t-1}, x_{t-2}, x_{t-3}, \dots, x_{t-n})$ and the output layer information are the predicted coordinates of the Bi-LSTM model in the line pans of the AFC at the t -th blade. According to the relationship between the cutting depth of the shearer and the structure of the line pan during the advancement of the fully mechanized mining face (the cutting depth of shearer is approximately equal to the width of three line pans), the time step is set to 3.

Based on the prediction task in this article, the number of layers for Bi-LSTM is set to 2, where the number of neurons in the first hidden layer is set to 250, the number of neurons in the second hidden layer is set to 30, the number of training sample sets is 1200, the learning rate is set in the range of [0.005,0.05], the maximum number of iterations is 1000, the gradient threshold is set as 1 to prevent gradient explosion, Dropout is used to reduce over-fitting, RMSE and MAPE are used as the loss function.

In order to achieve long-term prediction, this article adopts a rolling prediction method. After selecting a fixed time window of 3-blade data and training a time series model each time, the trajectory of the future 3-blade scraper conveyor is predicted. After prediction, the data from the same time window in the test set is added to the training set to continue training the model.

3.2 Data sources

In virtual simulation system, virtual positioning of shearer is carried out by means of virtual Strapdown Inertial Navigation System (SINS) and virtual odometer, and AFC trajectory is obtained by trajectory inversion. In this system, the sum of positioning error and inversion error of shearer is simulated by defining an arbitrary number, and the range is set ($error_min, error_max$). Given the absolute coordinate system of the virtual fully-mechanized mining face, the following functions are used to simulate the output of detection results when the position of line pan is detected by SINS.

```
gameobject_Position_x = this.transform.position.x + random;
gameobject_Position_y = this.transform.position.y + random;
gameobject_Position_z = this.transform.position.z + random;
```

The hydraulic support number in the virtual scene is $yyzz_num(num \in (1,n))$; The number of the line pan of the AFC is $zbc_num(num \in (1,m))$. Where, n is the number of hydraulic supports and m is the number of line pans. Through the above program, the position coordinates of each line pan are output in the format of xml in Unity3D, the displacement and yaw angle values of the pushing mechanism of the hydraulic support are output

in the same way, and imported into Matlab in the form of cell array as the data set of Bi-LSTM neural network prediction.

If the hydraulic support and the AFC advance continuously on the virtual floor, determine the advance times of the AFC according to the visualization of the creeping movement of the AFC in the scene. The track coordinates of the AFC after the completion of the last process in each propulsion process are used as the predicted data set. Due to the similarity between the cutting depth of the shearer and the pushing distance of the AFC, the overall running track of the adjacent two-blade of AFC is less affected by the overall fluctuation of the coal seam and has certain correlation, which will lead to the lag between the predicted value and the true value. In this paper, differential calculation is used to eliminate the autocorrelation.

3.3 Model Evaluation Index

Root Mean Square Error (RMSE) and Mean Absolute Percentage Error (MAPE) are used as the evaluation index of simulation deviation to reflect the degree of difference between measured and simulated values.

$$RMSE = \sqrt{\frac{1}{n} \sum_{i=1}^N (p_i - q_i)^2} \quad (17)$$

$$MAPE = \frac{1}{n} \sum_{i=1}^N \left| \frac{p_i - q_i}{p_i} \right| \quad (18)$$

where, n is the sample size, p_i and q_i are the predicted values and the predicted values of the track coordinates of the AFC respectively ($i=1\dots n$).

3.4 Model comparison

If the number of line pan and hydraulic support are both 40, the hydraulic support continuously pushes the AFC through 8 cycles with a total of 16×40 data. The 15th data set is used to forecast the 16th data set and the number of iterations is 250. Since the x-coordinate of AFC varies greatly with the fluctuation of coal seam, the two-difference method is used to process the most data set. In this paper, Bi-LSTM neural network and LSTM neural network are selected for comparative analysis. The difference between the predicted results and the actual values is shown in Fig. 4.

From the changes in the values of the indicators during training in Fig. 4(a)-(b) that the Bi-LSTM neural network has a better prediction and convergence level than the LSTM neural network in predicting the trajectory of the AFC. It can be seen from Fig. 4(d) that the prediction results of Bi-LSTM neural network fluctuate around the actual value curve and are relatively close to the fluctuation of the actual value curve; The LSTM neural network also fluctuates around the actual value curve, but the fluctuation is large; It can be seen from Fig. 4(e) that the area of the error value obtained by using LSTM neural network for prediction will be greater than that by using Bi-LSTM neural network, which shows that the error

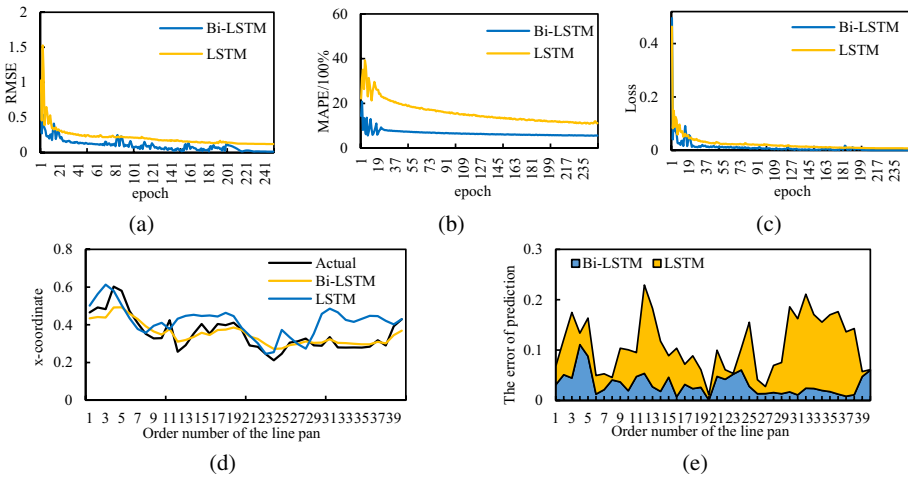


Fig.4 Prediction results

of LSTM neural network for prediction is large. In conclusion, the prediction accuracy of Bi-LSTM neural network is higher, so the prediction of Bi-LSTM neural network is reliable.

4 Judgment mechanism of the creeping degree of AFC based on fuzzy evidence reasoning theory

4.1 Pose determination of virtual AFC based on Rodrigues parameters

On the basis of obtaining the position coordinates of the AFC, it needs to be converted into the information that can virtually drive the AFC in Unity3D. The driving factor selected in this article is the relative deflection angle between adjacent line pans. Therefore, it is necessary to establish a conversion mechanism between the position coordinates and the deflection angle.

The Rodrigues parameter is a formula for calculating a new vector obtained by rotating a vector around the axis of rotation by a given angle in three-dimensional space. Therefore, when the two vectors before and after the rotation are known, the angle of rotation can be calculated. The calculation equation of Rodrigues parameter is shown in Eq. (19):

$$\varnothing = n \tan \frac{\alpha}{2} \tag{19}$$

where \varnothing is the Rodrigues parameter, α is the rotation angle of P_i around the rotation axis n , and n is the rotation axis. It can be seen from the formula that this method is prone to the problem of singular values (the rotation angle is $\pm 180^\circ$). However, due to the limitations of mining conditions and the structure characteristic of the AFC, the deflection angle of the line pan is generally not more than 4° , so this paper selects the Rodrigues parameter to solve the relative deflection angle between the line pans.

The position coordinate of the line pan A_i is represented by a vector $P_i(x_i, y_i, z_i)$, and the relative deflection angle between the two adjacent line pans is determined by calculating the angle

between the two adjacent vectors. On the premise of obtaining the vector representing the position of each line pan of the AFC, the vertical axis of the Character Joint component is used as the rotating axis n . The relative deflection angle between two adjacent line pans is determined by the relative rotation between the two vectors P_i and P_{i+1} and can be expressed by Eq. (20).

$$P_{i+1} = P_i + \frac{1}{1 + \varnothing^2} [\varnothing \times P_i + \varnothing \times (\varnothing \times P_i)] = RP_i \tag{20}$$

where \varnothing is the module of the Rodrigues parameter and R is the rotation matrix expressed by the Rodrigues parameter from P_i to P_{i+1} . The expression of the rotation matrix is shown in Eq. (21).

$$R = \frac{1}{1 + \varnothing^2} \begin{bmatrix} 1 + \varnothing_x^2 - \varnothing_y^2 - \varnothing_z^2 & 2(\varnothing_x\varnothing_y - \varnothing_z) & 2(\varnothing_x\varnothing_z + \varnothing_y) \\ 2(\varnothing_x\varnothing_y + \varnothing_z) & 1 - \varnothing_x^2 + \varnothing_y^2 - \varnothing_z^2 & 2(\varnothing_y\varnothing_z - \varnothing_x) \\ 2(\varnothing_x\varnothing_z - \varnothing_y) & 2(\varnothing_y\varnothing_z + \varnothing_x) & 1 - \varnothing_x^2 - \varnothing_y^2 + \varnothing_z^2 \end{bmatrix} \tag{21}$$

Set the difference of Euler angle between the line pan A_{i+1} and A_i to be the yaw angle $\Delta\varphi$, pitch angle $\Delta\theta$, roll angle $\Delta\gamma$, then the relation between euler angle and Rodrigues parameter is shown in Eq. (22):

$$\varnothing = \frac{1}{1 + \tan \frac{\Delta\varphi}{2} \tan \frac{\Delta\theta}{2} \tan \frac{\Delta\gamma}{2}} \begin{bmatrix} \tan \frac{\Delta\gamma}{2} - \tan \frac{\Delta\varphi}{2} \tan \frac{\Delta\theta}{2} \\ \tan \frac{\Delta\theta}{2} + \tan \frac{\Delta\varphi}{2} \tan \frac{\Delta\gamma}{2} \\ \tan \frac{\Delta\varphi}{2} + \tan \frac{\Delta\theta}{2} \tan \frac{\Delta\gamma}{2} \end{bmatrix} \tag{22}$$

The difference of euler angle between line pan A_{i+1} and A_i is obtained as Eq. (23).

$$\begin{cases} \tan\Delta\varphi = \frac{2(\varnothing_x\varnothing_y - \varnothing_z)}{1 - \varnothing_x^2 + \varnothing_y^2 - \varnothing_z^2} \\ \sin\Delta\theta = \frac{2(\varnothing_y\varnothing_z + \varnothing_x)}{1 + \varnothing^2} \\ \tan\Delta\gamma = \frac{-2(\varnothing_x\varnothing_z - \varnothing_y)}{1 - \varnothing_x^2 - \varnothing_y^2 + \varnothing_z^2} \end{cases} \tag{23}$$

4.2 Evaluating the creep degree based on Fuzzy Comprehensive Evaluation method

4.2.1 Triangular fuzzy numbers

In order to better describe the fuzzy variable of the degree of the creeping of the AFC, this paper uses triangular fuzzy numbers to describe the degree of equipment creeping. Triangular fuzzy numbers have the characteristics of simple construction and easy operation in the process of expressing fuzzy semantics (Bowen et al. 1992). Its writing form is (x, y, z) , where x, y and z represent the left end point, midpoint and right end point of fuzzy number respectively. The operation rules are as follows:

$$l_1A + l_2B = (l_1 \cdot x_1 + l_2 \cdot x_2, l_1 \cdot y_1 + l_2 \cdot y_2, l_1 \cdot z_1 + l_2 \cdot z_2) \tag{24}$$

where $A = (x_1, y_1, z_1)$, $B = (x_2, y_2, z_2)$. Take A as an example to describe the membership function:

$$\mu_A(x) = \begin{cases} \frac{x-x_1}{y_1-x_1}, x \in [x_1, y_1] \\ \frac{y_1-x_1}{z_1-y_1}, x \in [y_1, z_1] \\ 0, x \notin [y_1, z_1] \end{cases} \tag{25}$$

In order to realize the quantitative comparison between different degrees, it is necessary to defuzzify the evaluation results when determining the degree of creeping of AFC. In this paper, barycenter method is used for defuzzification, as shown in Eq. (26).

$$\bar{x}_0(A) = \frac{\int_{x_1}^{z_1} x\mu_A(x)dx}{\int_{x_1}^{z_1} \mu_A(x)dx} \tag{26}$$

4.2.2 Fuzzy Comprehensive Evaluation

In response to the problem of subjective influence on numerical evaluation when judging the degree of creeping of AFC, the fuzzy comprehensive evaluation method is adopted to make up for it in this paper. The process is as follows: Firstly, based on the evaluation method of fuzzy mathematics, the quantitative evaluation of the degree of creeping is fuzzified to form a fuzzy terminology set; Secondly, conduct fuzzy evaluation and obtain fuzzy conclusions through fuzzy reasoning; Finally, defuzzification is performed to obtain the risk priority number RPN.

The Risk Priority Number (RPN) is used to evaluate the degree of the accident. The higher its value is, the more serious the consequence of the accident is. The calculation equation of RPN is:

$$RPN = ESR \times OPR \times DDR \tag{27}$$

where, *ESR* (Effect Severity Ranking) is the severity level of the accident, *OPR* (Occurrence Probability Ranking) is the probability of the accident and *DDR* (Detection Difficulty Ranking) is the difficulty of the accident detection.

According to the research on the creeping of AFC in the existing engineering cases(V Xu 1999; Verma 2013; Wang et al. 2020), the creeping degree of AFC in the virtual environment is quantified as the ratings VL, L, M, H and VH, which indicate Very Low, Low, Medium, High and Very High. The final established fuzzy rating and corresponding fuzzy numbers are shown in Table 3, where P_A is the probability of corresponding degree of the creeping of AFC.

4.2.3 Schematic diagram of the degree of creeping of the AFC

Figure 5 shows the corresponding creep degree diagram of AFC in Table 3, in which Fig. 5(a) shows the scene when AFC is operating normally. Figure 5(b) shows that the degree of creeping on AFC is VL, and the creeping on AFC can hardly be judged by naked eyes, requiring special high-precision positioning device to determine; Fig. 5(c) shows that the degree of creeping on AFC is L. At this time, the creep of AFC is small and the position change is difficult to judge compared with reference datum, so traditional sensor positioning device is needed to detect it. Figure 5(d) shows that the creeping degree of the AFC is M. at this time, the position of the AFC changes greatly, and the equipment is separated from the roadway, which can be clearly judged by the naked eye; Fig. 5(e) shows that

Table 3 Evaluation chart of AFC's creeping

Rating	Fuzzy number	ESR	OPR	DDR
VL	(1,1,3)	The whole working face can run normally	$P_A \geq 10^{-1}$	Sensor positioning devices requiring high precision for detection
L	(1,3,5)	The production is slightly affected and the mining process needs to be adjusted during mining	$10^{-2} \leq P_A \leq 10^{-1}$	Traditional sensing positioning devices are required for detection
M	(3,5,7)	The production is moderately affected, it is necessary to stop the machine and carry out relevant adjustment	$10^{-4} \leq P_A \leq 10^{-2}$	Can be judged by the human senses
H	(5,7,9)	There is a high probability of mining accidents	$10^{-6} \leq P_A \leq 10^{-4}$	Easily judged by the human senses
VH	(7,9,9)	Equipment accumulation occurs in comprehensive mining face and major mining accidents occur	$P_A \leq 10^{-6}$	It is very easy to judge directly by human senses

the creeping degree of the AFC is H, at this time, the head position of the AFC has been completely separated from the roadway, and the tail tends to accumulate in the roadway; Fig. 5(f) shows that the creeping degree of the AFC is VH. At this time, it is very easy to observe with the naked eye, and the equipment has been stacked.

4.3 Evaluation indicators for creeping of AFC based on equipment movement

4.3.1 The motion of floating connection mechanism (F)

Because the connection between the hydraulic support and the AFC is a floating connection mechanism, when the AFC is creeping, the mechanism will deflect along with the key points on the line pan, and the moving direction of the AFC is consistent with the deflection direction of the push rod of the floating connection mechanism. Whether the AFC creeps can be judged according to the specific motion parameter values of each structure of the floating connection mechanism. For example, when the direction of the relay bar is deflected downwards, it indicates that the AFC has downslide.

4.3.2 Reference position deviation of AFC (D)

As shown in Fig. 5, it is a schematic diagram of the creep of the AFC during operation, in which the yellow line represents the edge line of the roadway, the white line represents the position of the head when the creep movement does not occur, and the red line represents the actual position of the head. When the AFC creeps, select a key part of the AFC as the reference standard to determine whether the AFC creeps according to the position change of the part. As the head and tail of the AFC, the position change of the head and tail is easier to obtain than that of other line pans, so one of them can be selected as the reference position for the creep of the AFC.

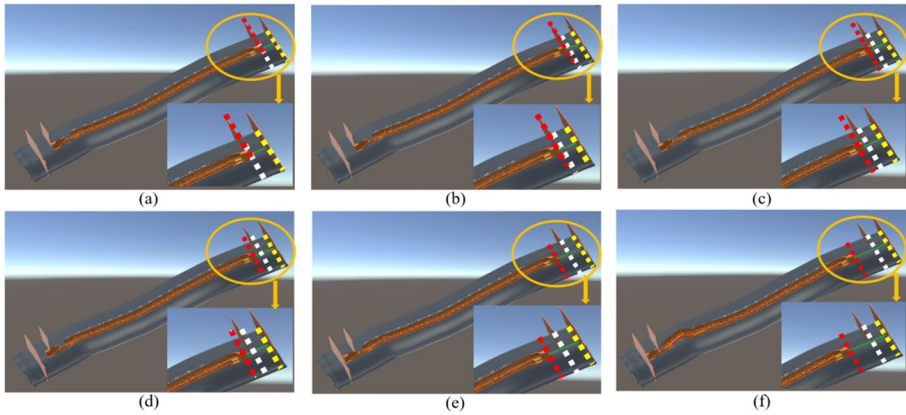


Fig. 5 Degree of the creeping of AFC

4.4 Judgment method of creeping degree of virtual AFC based on D-S evidence theory

4.4.1 Evaluation of the degree of creeping based on D-S evidence theory

According to the evaluation grade of the creeping degree of the AFC, the identification framework Ω of D-S evidence theory (Dempster 1967, 1968; Shafer 1976) is established, as shown in the following Eq. (28):

$$\Omega = \{H_1, H_2, H_3, H_4, H_5\} \tag{28}$$

where, $H_i (1 \leq i \leq 5)$ represents the evaluation level of the creeping degree of the AFC of the current blade, which is VL, L, M, H, VH.

Let the evidence set be $F_i (i=1,2)$, where F_1 represents the displacement d of the AFC and F_2 represents the deflection φ of the floating connection mechanism. Based on the evaluation indicators (F, D), the range of creeping rate (d_0^i, d_1^i) and the range of yaw angle (φ_0^i, φ_1^i) of the floating connection mechanism corresponding to each level were preliminarily deduced through simulation and rehearsal in a virtual environment. Establish the basic probability allocation function for each evaluation level based on the established identification framework, which is the mapping shown in Eq. (29), also known as the m function (Shafer 1976), where $m : 2^\Omega \rightarrow [0, 1]$. Establish the m function for two pieces of evidence on the Ω .

$$\begin{cases} m_j(H_i) = \frac{c_{ji}}{\sum_{i=1}^5 c_{ji} + (1-k_j)} \\ m_j(E) = \frac{(1-k_j)}{\sum_{i=1}^5 c_{ji} + (1-k_j)} \\ \sum_{i=1}^5 m_j(H_i) + m_j(E) = 1 \end{cases}, 1 \leq j \leq 2, 1 \leq i \leq 5 \tag{29}$$

The set $E = H_1 \cup H_2 \cup H_3 \cup H_4 \cup H_5$ represents the inability to determine the current level of creeping. Let m_1 is the m function of F_1 on Ω , where k_1 is the reliability parameter of F_1 , and $c_{1i} = (d/(d_0^i + d_1^i)) / \sum_{i=1}^5 (d/(d_0^i + d_1^i))$; m_2 is the m function of F_2 on Ω , k_2 is the reliability parameter of F_2 , and $c_{2i} = (\varphi/(\varphi_0^i + \varphi_1^i)) / \sum_{i=1}^5 (\varphi/(\varphi_0^i + \varphi_1^i))$.

The basic probability distribution function satisfies the following two conditions in Eq. (30), where $m(a)$ represents the degree of support for event a :

$$\begin{cases} m(\emptyset) = 0 \\ \sum_{a \in \Omega} m(a) = 1 \end{cases} \tag{30}$$

This article uses an improved Yager formula (Yager 1987) for function synthesis. For specified events and other unknown propositions, function synthesis is performed according to Eq. (31):

$$\begin{cases} m(a) = p(a) + k \cdot \varepsilon \cdot q(a), a \neq \emptyset, \Omega \\ m(\Omega) = p(\Omega) + k \cdot \varepsilon \cdot q(\Omega) + k(1 - \varepsilon) \end{cases} \tag{31}$$

where, $k = \tilde{k} = 2/n(n - 1) \sum_{i < j \leq n} k_{ij}$, $k_{ij} = \sum_{a_i \cap a_j = \emptyset, a_i \in F_1, a_j \in F_2} m_i(a_i) m_j(a_j)$ is the conflict value between the evidence set F_1 and F_2 , $p(a) = \sum_{a_i \in F_i, \bigcap_{i=1}^n a_i = \Omega} m_1(a_1) \dots m_n(a_n)$, $q(a) = 1/n \sum_{i=1}^n m_i(\Omega)$, $\varepsilon = e^{-k}$.

4.4.2 Virtual decision making of creeping degree of AFC

Based on the content of the above chapters, the prediction method in Sect. 3 is used to predict the position track of the AFC, and the evaluation grade, triangular fuzzy number and accident evaluation results are preliminarily determined according to the virtual conversion results of the predicted track. On the basis of the evaluation results obtained and virtual visualization of prediction results achieved, two coal miners are invited to conduct a secondary evaluation according to their work experience, evaluation indicators (F, D) based on the predicted trajectory of the AFC as the evidence set of reasoning. The final decision-making result of the creeping degree of the AFC is obtained is shown in Eq. (32).

$$S = S_1 \times S_2 \times S_3 = \{f(s_1, s_2, s_3) | s_i \in S_i, i = 1 \dots 3\} \tag{32}$$

where S is the result of synthesis using Yager formula, and the value range of membership function is between $[0, 1]$. The closer the result is to 1, the higher the support for the decision; $S_i (i = 1, \dots, 3)$ respectively represent the preliminary evaluation results obtained based on the prediction results, the expert's work experience, and the results obtained from the evaluation indicators (F, D); s_i stands for results in S_i . Based on the decision results, if there is an creeping trend, on the basis of determining the degree of the accident, timely process adjustments should be made to ensure safe production or minimize losses; If not, coal mining can continue according to the original process.

5 Experimental research

Under the analysis of the single factor influencing the creeping of the AFC in Sect. 2.2, the single factor influencing the creeping of the AFC is analyzed first. By building a test platform for the creeping of the AFC in the laboratory environment, the impact of each factor on the creeping of the AFC is tested in the virtual environment and the laboratory environment respectively, which proves the reliability of the virtual simulation analysis system. Then the 9711 high mining height fully- mechanized working face of a group *KaiYuan*

mine is selected for research. According to the historical operation information of the AFC, the degree of the creeping of the AFC in the process of propulsion is judged.

5.1 Reliable verification of virtual simulation system for analyzing the creeping of AFC

5.1.1 Virtual simulation system for analyzing the creeping of AFC

As shown in Fig. 6, the virtual monitoring control panel mainly includes Data input area, Action control area, Data storage area, Input preparation area and Scene monitoring area, and uses the predicted trajectory established in Sect. 4 to conduct virtual conversion of the predicted trajectory of the AFC in Unity3D. The data interface is reserved in the C# script, and the established factor allocation scheme is input into the parameter setting area of the system interface, so that the research environment can be configured, including the inclination of the support, the inclination of the AFC, the inclination of the coal seam, the friction factor, the Drag, the Angular Drag, and the acting force of the coal miner, including inclination of hydraulic support, inclination of AFC, inclination of floor, friction factor, Drag, Angular Drag, force of shearer. On the basis of virtual connection between hydraulic support and AFC, virtual infrared ranging sensor is installed at the head of AFC. The position of AFC can be monitored during pushing and the relative position of head and tunnel can be output in real time.

5.1.2 Parameter configuration of virtual simulation system

During the process of sliding from static to dynamic of AFC, combined with the influence of water spraying and dust during running of shearer, there is a conversion of friction coefficient between equipment and floor. In order to accurately describe this friction process,

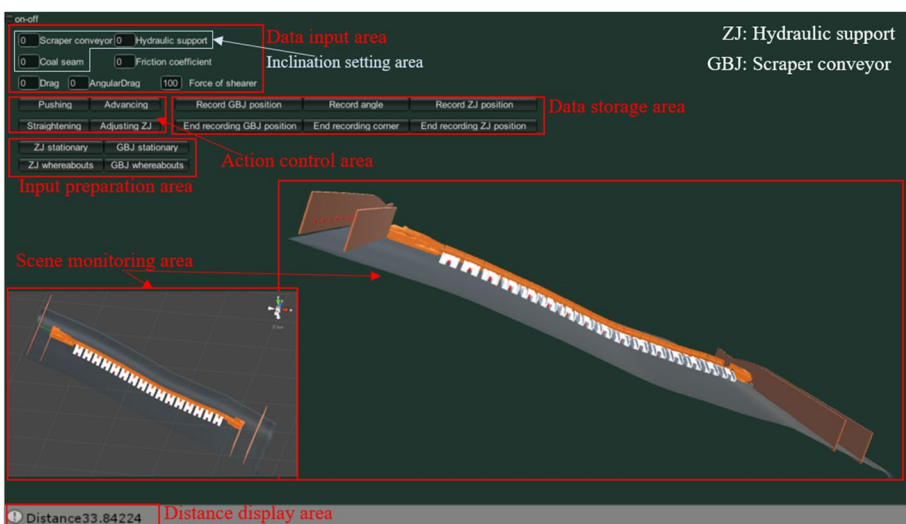


Fig. 6 Interface of virtual simulation subsystem for influencing factor analysis of the creeping of AFC

Stribeck friction model is used to determine the friction coefficient between the line pans and the floor.

$$f = f_D + (f_S - f_D)e^{-\left(\frac{v_s}{v_{st}}\right)^2} \tag{33}$$

where f_D is the dynamic friction factor, f_S is the static friction factor, v_s is the running speed of the AFC and v_{st} is the critical Stribeck speed. In this paper, the simulation parameters of v_s and v_{st} are set as 1 m/s and 0.001 m/s respectively.

In order to establish the mapping relationship between coal machine equipment in virtual environment and coal machine equipment in physical environment (Guo et al. 2019), it is necessary to establish virtual mapping of physical parameters of equipment in Unity3D to get the digital twin of "Three Machines" in comprehensive mining face. Setting the environmental parameters according to Table 4.

5.1.3 Construction of test platform

As shown in Fig. 7, this experiment takes the fully-mechanized mining face prototype platform (Fig. 7(a)) under the laboratory environment as the experimental research platform. The whole platform is composed of hydraulic support prototype model, adjustable floor model (Fig 7(c)), AFC model and fixed floor model (Fig. 7(d)). Due to the limited number of prototype models of hydraulic support in the laboratory, this experiment cannot be completed, therefore, this experiment adopts a straight wooden stick with flattened and the same four sides. According to the principle of centering with the line pan, a rope is tied at the cable trough between the wooden stick and the prototype of the line pan. As shown in Fig. 7(b), the prototype of the AFC is pushed by rotating the wooden stick. The fluctuation of adjustable floor model can be changed by adjusting the height of sliding trough and by laying different layers of friction coefficient on the base of prototype. The operating resistance between the two adjacent line pans of the AFC model can be changed by adjusting the tightness of the connections.

Install the infrared distance sensor module in the No. 1 line pan and simulate the tunnel with the side of the carton. By monitoring the relative distance between the line pan of the sensor and the simulated tunnel during the process of pushing the AFC by the hydraulic support, it can be judged whether the prototype of AFC has crept.

Table 4 Virtual parameter settings and functions

Parameter	Parameter change mode	Effect
Friction factor	The friction is set by means of Physical Material component, and the friction coefficient value is calculated by Eq. 33	Changing friction coefficient between virtual coal floor and coal machine equipment
Gravity of equipment	Use the Rigidbody class to modify the quality values of each equipment	Ensure that the equipment movement process has mechanical properties
Operating resistance	Using Angular Drag and Drag units to set the resistance of the line pan.	The Angular Drag unit is used to prevent the object from rotating. The Drag unit is used to obstruct the movement of an object

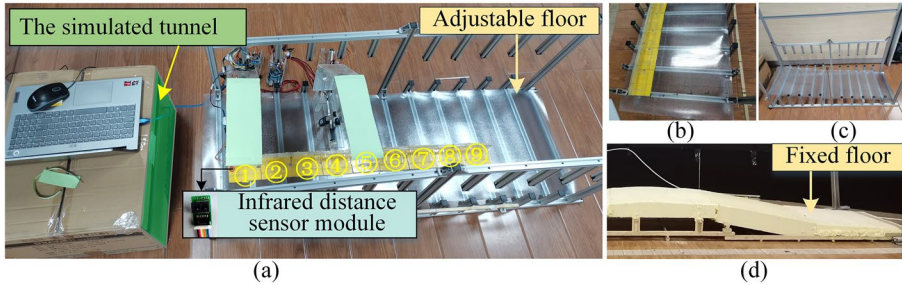


Fig. 7 Test device

5.1.4 Reliability analysis of virtual simulation system

(1) Experimental scheme

Input the parameter values in the scheme as shown in the Table 5 at the monitoring panel in the virtual environment for test respectively. The initial scheme value of each affected parameter value is (15° , 0.35, 500N, 1.5, 15) to ensure that the equipment can operate normally without virtual test. When a single factor is tested according to the scheme in the table, other values in the initial scheme value remain unchanged.

Due to the limitation of laboratory conditions, only limited resources can be used for this test. The test scheme is shown in Table 6.

The experimental design scheme is shown in Fig. 8, in which Fig. 8(a) is the undulation setting scheme along the coal seam strike, Fig. 8(b) is the friction factor setting scheme between equipment and coal seam floor, Fig. 8(c) is the dip angle setting scheme of coal seam, and Fig. 8(d) is the angular resistance setting scheme.

(2) Experimental result

As can be seen from Fig. 9(a), under the condition of the same average coal seam inclination angle, when there is no fluctuation, the position change is relatively large, indicating that the creeping phenomenon of the AFC is relatively serious; On the contrary, the position of the head hardly changes, which shows that the fluctuation of the coal seam floor along the coal seam strike will weaken the degree of the creep of the AFC. The relative distance at point 7 shows a non-linear relationship with the number of advances, as the mesh stitching is not smooth enough during virtual coal seam modeling, resulting in slight protrusions in the virtual coal seam.

As can be seen from Fig. 9(b), through the comparison of the two curves, it is found that with the advancement of the AFC, the data fluctuation increases, it is due to the vibration of the sensor module and the fluctuation of coal seam, but the relative distance of S1 is gradually greater than S2, which is consistent with the conclusion in Fig. 9(a).

As can be seen from Fig. 10(a), with the increase of friction coefficient, the position of AFC becomes more stable. When the friction coefficient is within the range of (0.3,0.5), the final relative distance between AFC and roadway benchmark changes very little during the propulsion, and the operation state of AFC is relatively stable;

Table 5 Virtual test scheme

No	The undulation of virtual coal seam	Inclination angle of Coal Seam (°)	Friction coefficient	Angular Drag
1	No fluctuation along the coal seam strike (V1)	10	0.1	0
2		15	0.2	0.5
3	There is fluctuation along the coal seam strike(V2)	20	0.3	1
4		25	0.4	1.5
5		30	0.5	2

As can be seen from Fig. 10(b), the coarser the surface material of the coal seam, the smaller the relative distance between the infrared ranging sensor module and the simulated roadway, and the smaller the amount of the creep of the AFC, which shows that when the friction coefficient between the floor and the AFC is greater, the AFC is less likely to creep. In the coal mine, the friction coefficient of the floor to the coal machine equipment is 0.35–0.40, which is basically consistent with the above conclusions, which proves the effectiveness and feasibility of the simulation test in the virtual environment.

It can be seen from Fig. 11(a) that the final relative distance between AFC and roadway datum increases by an average of 0.3 dm with the increase of coal seam dip, when the inclination angle of coal seam exceeds 15°. In Fig. 11(b), as the number of nuts increases, the final relative position between the AFC and the simulated tunnel increases by an average of 2.5 cm. It can be seen that whether in the virtual environment or in the laboratory environment, with the increase of coal seam inclination, the amount of the creep of AFC gradually increases. This is consistent with the conclusion that the dip angle is more likely to cause the AFC to creep due to the influence of the coal seam basement in the actual mining process, proving that the analysis of relevant experiments by the virtual simulation system is feasible.

As can be seen from Fig. 12(a), the relative creeping amount of the AFC is about 0.1 dm for every 1N reduction in Angular Drag; When the Angular Drag value is between (1.5, 2), the

Table 6 Laboratory test scheme

Factors	Test scheme	Parameter setting
The undulation of coal seam	Setting up two types of coal seams with and without undulations along the coal seam strike	S1: No undulation; S2: Undulation
Friction coefficient	M1 is the rough surface of plastic film, M2 is the smooth surface, M3 is the surface of fixed coal seam floor made of foam	Material friction coefficient of three kinds of coal bed pavement is $M3 > M1 > M2$
Inclination of coal seam	Nuts are placed on the side pad near the simulated roadway under the adjustable coal seam base, and the coal seam inclination is changed by changing the number of nuts	The tests are represented by $A_i (i = 0, 1, 2, 3)$, i refers to the number of nuts
Angular drag	Control of angular resistance between adjacent line pans by adjusting the tightness of the connection between adjacent line pans	C1: tight connection between adjacent two line pans; C2: loose connection

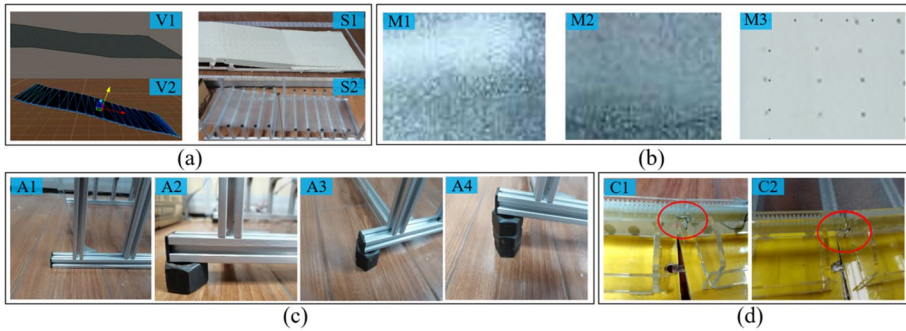


Fig. 8 Scheme setting

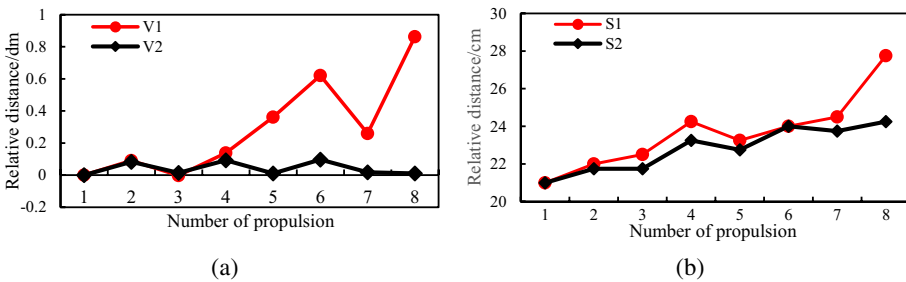


Fig. 9 Test results

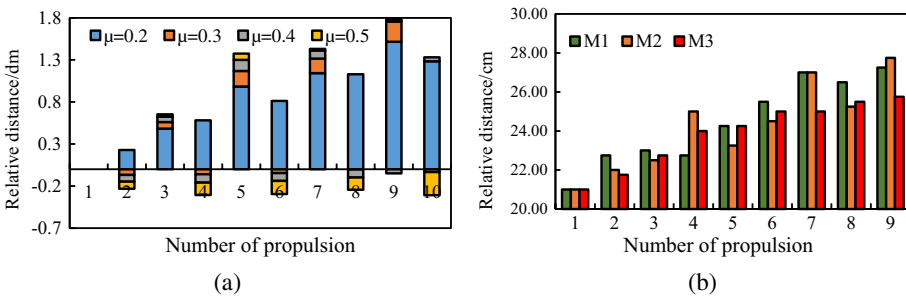


Fig. 10 Test results

position of the AFC tends to be stable when moving. As can be seen from Fig. 12(b), when the Angular Drag is small, the relative distance between the AFC and the simulated roadway is large. In summary, the greater the Angular Drag, the smaller the impact on the creeping of the AFC, and the straightness of AFC is easier to maintain and less prone to movement. This phenomenon corresponds to actual production conditions, proving the reliability of conducting simulation experiments in a virtual environment.

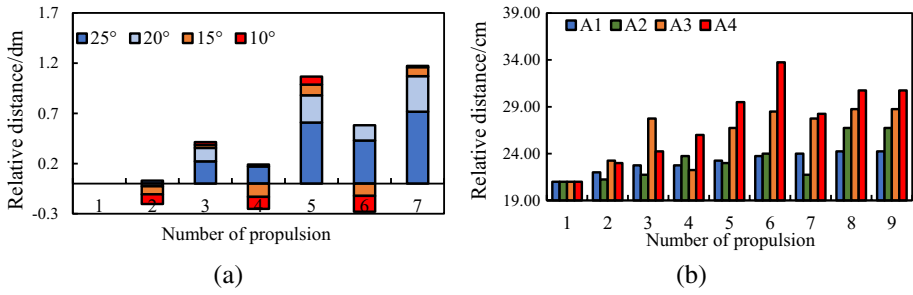


Fig. 11 Test results

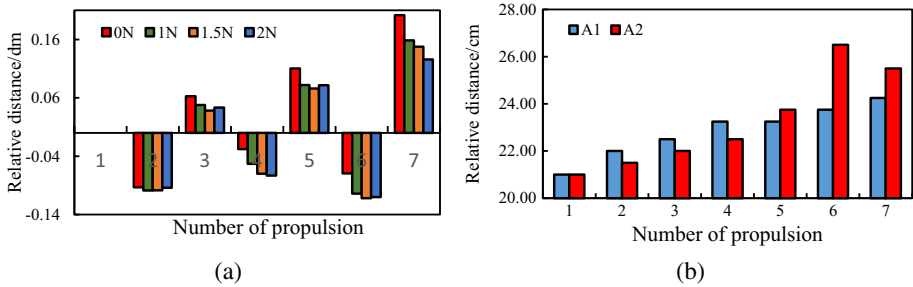


Fig. 12 Test results

5.2 Determination of creeping of the AFC for virtual fully-mechanized mining face with large mining height

After overcoming the key technologies, based on the Digital Twin theory, a targeted virtual simulation analysis system can be established to analyze the influencing characteristics of each factor and the priority of influencing degree among the factors. And when the parameters of each influencing factor are known, the virtual environment is specially configured to predict the development degree of the engineering problem of the creeping of AFC in actual production process.

9711 fully-mechanized mining face with large mining height in *Kaiyuan* Mine of a group was selected for study. The depth of the fully-mechanized working face is 364~417 m, with an average of 390.5 m, the strike length of the working face is 462 m, and the inclined length is 220 m. There are 4 mining roadways in the working face, i.e. air inlet, air return, low and high, and the roof is managed by the full-height mining technology with large mining height and full-collapse method. MG750/1900-GWD shearer and ZY8000/26/56D hydraulic support are used in the working face with a center distance of 1.75 m. During the initial mining of 9711 working face, there is bottom coal left, and the upper bottom coal is thicker, the lower bottom coal is thinner, the height difference between upper and lower lanes is small, the height difference between return lane and inlet lane is 20.7 m, the average angle of working face is 5.4 degrees, and the maximum angle is 10°, as shown in Fig. 13.

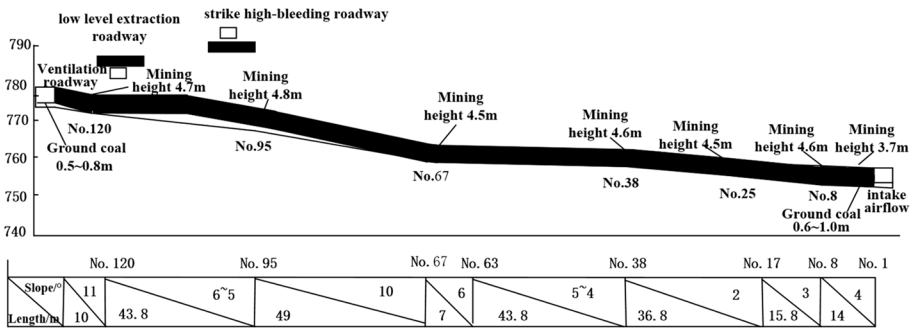


Fig. 13 Profile of 9711 fully-mechanized mining face

Due to the long working face strike length, the amount of data is large when analyzing and studying the creeping of AFC. This paper chooses the data of the line pan of the two process sections nearest the tail of the return lane for analysis, i.e. the data of the 16 line pans connected with the tail. Determine whether the AFC has slipped up or down by judging the position of the tail.

5.2.1 Virtual monitoring subsystem for creeping of the AFC in 9711 working face

(1) Fuzzy grey correlation analysis of the influencing factors of creeping of AFC

According to the content of Sect. 2.3, the friction coefficient $X_1\{k\}$, coal seam inclination $X_2\{k\}$, shearer force $X_3\{k\}$, Angular Drag value $X_4\{k\}$, Drag value $X_5\{k\}$ were compared with the creeping limit value $Y\{k\}$ of the creeping amount. The results between each comparison sequence and the reference sequence are shown in Table 7.

From Table 7, it can be seen that the priority factors affecting the creeping of AFC in the virtual environment are: Shearer force, Angular Drag value, Inclination angle of coal seam, Friction coefficient, and Drag value. In order to make decisions on the degree of creeping of AFC in a virtual environment, it is necessary to configure the propulsion environment of the AFC based on the priority of the influencing factors obtained.

(2) Parameter settings for virtual monitoring subsystem

Table 7 Fuzzy grey relational analysis table of influencing factors the creeping of AFC

Factors	C1	C2	C3	C4	C5	Relevancy
Friction coefficient	6.4052	1.5588	0.1820	0.0473	0.1909	0.7789
Inclination angle of coal seam	2.94069	0.71658	0.3544	0.0898	0.0115	0.7828
Shearer force	0.8340	0.8348	0.7423	0.6571	0.5660	0.9515
Angular Drag	0.2016	0.1820	0.1584	0.1476	0.1257	0.9288
Drag	0.1197	0.3833	0.5379	0.6729	0.6962	0.5213
Creeping limit value	0.1	0.1	0.1	0.1	0.1	

As shown in Fig. 14, the interface of the virtual monitoring subsystem for the creeping of the AFC in the 9711 working face is shown. The virtual monitoring subsystem has the same function as the virtual simulation subsystem for the analysis of the factors affecting the creeping of the AFC. In the subsystem, there are 120 hydraulic supports, 120 line pans (including head and tail). In the virtual environment, the horizontal bending resistance and transverse bending resistance are 1.460 N and 2.480 N respectively. In Unity3D, the Angular Drag value is 3.940 N. Under the virtual environment, the drag value of the AFC is 19.334 N, the friction factor is 0.35, the single motor cutting power of the shearer is 750 KW, and the total power is 1900 KW.

5.2.2 Prediction of the propulsion trajectory of the virtual AFC

The mining height of 9711 fully mechanized working face is relatively high and the coal seam strength is low. According to the environmental parameters determined in Sect. 5.2.1, without any interference with the advance state of the AFC, the AFC can be continuously advanced for 6 cycles, and the position of the head will be output in the form of an xml file in real time during the advance process. In the process of propulsion, the position of the head is output in the form of an xml file in real time. After the number of cutters is filtered by propulsion, the filtered data is processed again using the difference method, and the built Bi-LSTM network is used for prediction. The prediction results are shown in Fig. 15.

It can be seen from Fig. 15(a) that the prediction accuracy of the AFC trajectory by using this prediction algorithm is high, the maximum error is 0.2, the RMSE value is 0.085783, and the MAPE value is 0.242512. It can be seen from Fig. 15(b) that the predicted three-dimensional trajectory of the AFC almost coincides with the converted observation trajectory, indicating that the reliability of Bi-LSTM in predicting the AFC trajectory is high.

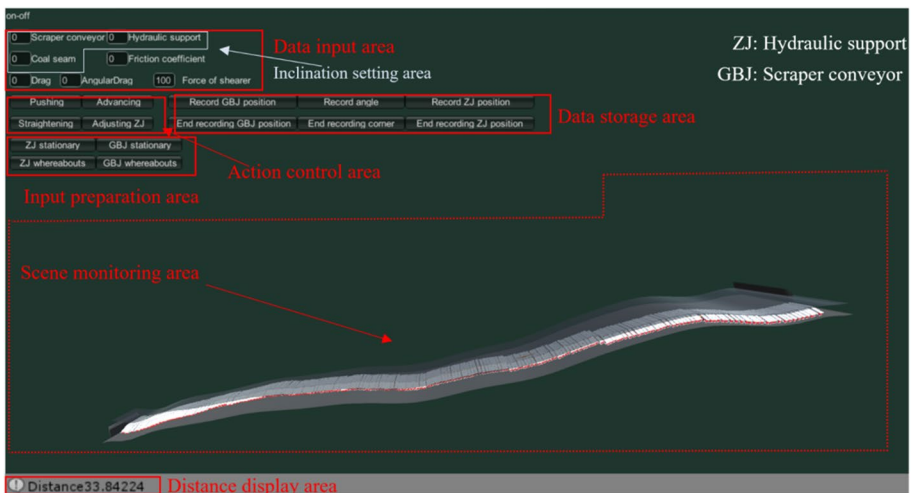
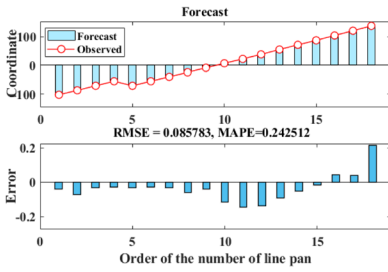
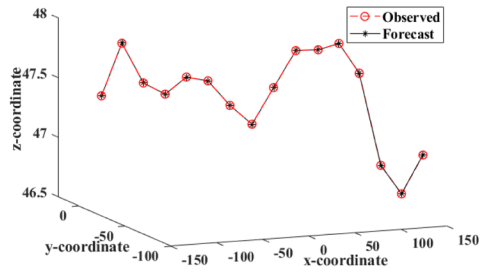


Fig. 14 Interface of virtual monitoring subsystem for the creeping of AFC in 9711 working face



(a) Track of moving direction of AFC



(b) Three dimensional trajectory of AFC

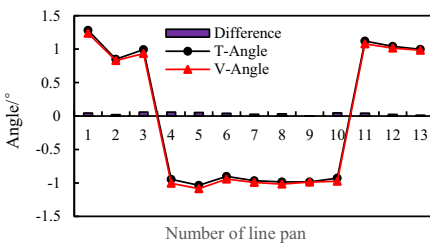
Fig. 15 Trajectory of AFC

5.2.3 Determination of the creep degree of the AFC

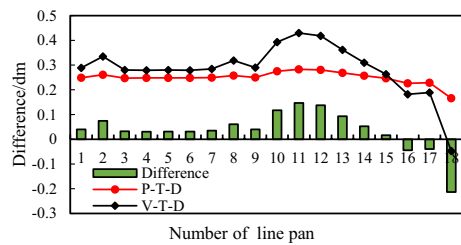
Convert the predicted track into the rotation angle of the line pans according to Sect. 4.1, and control the rotation of each line pan through C# script. The obtained track curve is shown in Fig. 16(b). According to the x-coordinate value of the AFC, the creep degree can be determined. In this paper, only the x-coordinate part is intercepted for research.

The calculated deflection angle (T-Angle) and the deflection angle (V-Angle) of the virtual transformation of the predicted trajectory are shown in Fig. 16(a). The difference between the theoretical calculation angle and the angle after virtual application is within 0.9°, and the accuracy is 87.1%; The x-coordinate value of the predicted trajectory after virtual application and the x-coordinate value of the predicted trajectory are differentially processed with the x-coordinate of the previous trajectory, and the obtained trajectory curves are recorded as (P-T) and (V-T) respectively. The difference between the predicted trajectory and the virtual trajectory is within 0.2 dm. This shows that the application accuracy of the virtual transformation model in Sect. 4.1 is high.

According to the predicted AFC trajectory, the comparison with the initial trajectory is obtained as shown in Fig. 17(a) shows the comparison between the predicted trajectory (P-T) and the virtual converted trajectory (V-T) of the predicted result and the initial trajectory (I-T) of the AFC. Figure 17(b) shows the comparison between the implied channeling momentum (D-C-P) in the virtual track and the implied channeling momentum (D-C-V) in the virtual transition track. It can be seen that the difference between the two tracks is within 0.2 dm, which indicates that it is feasible to determine the creeping degree of AFC



(a)



(b)

Fig. 16 Virtual transformation results

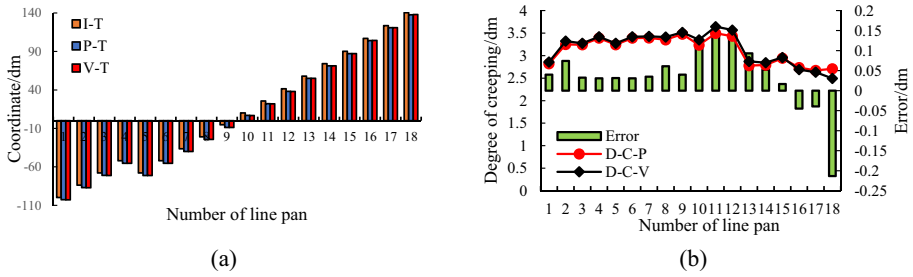


Fig. 17 Virtual transformation results

using the virtual transition track. The channeling momentum can be described by using the fuzzy number (5, 7, 9) and the preliminary judgment grade is H.

According to the results of virtual conversion, the specific movement parameters of each degree of freedom of the floating connection mechanism are obtained as shown in Fig. 18, where A1 and A2 respectively represent the yaw angle and pitch angle of the relay bar, A3 represents the yaw angle of the connection head, D1 represents the amount of displacement, Si (i = 1...16) represents the serial number of the hydraulic support, and its own experience determines the extent of creeping. From Fig. 18, it can be seen that the deflection angles A1 and A2 of the relay bar are both positive, which indicates that the relay bar is swaying downwards along the inclination direction of the seam floor, and the value A3

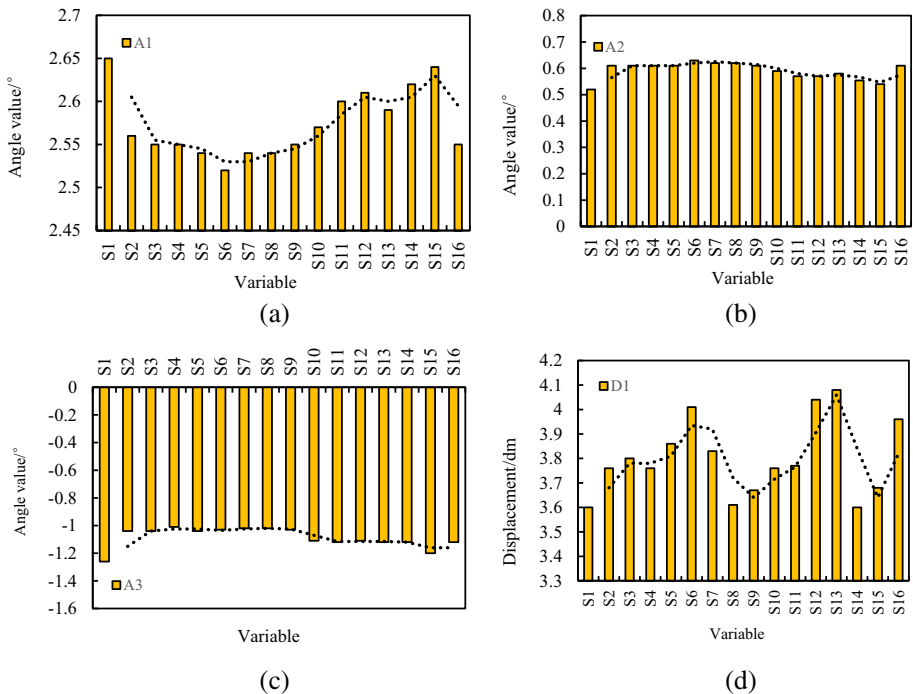


Fig. 18 Variation of motion parameters of the floating connection mechanism

Table 8 Evidence for evidence of the creeping of AFC

Results	V	L	M	H	VH
Pro1	0	0.01	0.02	0.94	0.03
Pro2	0	0.01	0.01	0.96	0.02

is positive, indicating that the deflection direction of the connection head is the same as that of the relay bar. The piston rod extension indicates that the hydraulic support is on the push AFC without the shift frame. These four factors comprehensively explain that during the process of pushing the AFC by the hydraulic support, the AFC is creeping and needs to stop for inspection according to experience.

According to the content of Sect. 4, referring to the predicted momentum of the AFC track and the movement results of the floating connection mechanism, the extent of the creep of the AFC is judged and the result shown in Table 8 is obtained.

From Table 8, the following synthesis results are obtained: $S(VL) = 10^{-4}$, $S(L) = 2 \times 10^{-4}$, $S(M) = 0.007801$, $S(H) = 0.9024$, $S(VH) = 6 \times 10^{-4}$. It can be seen that the degree of support for rating H is relatively high. Therefore, it can be considered that the extent of creeping on the AFC is H. There is a high probability of coal mining accidents. Emergency shutdown is required and measures are taken to prevent the AFC from continuing to creep and to avoid property damage caused by equipment accumulation.

5.3 Discussion

- (1) From the experimental results, it can be seen that the trend of the virtual simulation experiment is basically consistent with that of the laboratory experiment, which shows that it is feasible to analyze the creeping of the AFC through the virtual simulation system created in this paper to a certain extent. However, due to the limitation of experimental conditions, there is a certain gap between the test bench and the actual mining environment in the laboratory environment, and only qualitative analysis can be made on the creeping of the AFC.
- (2) The trajectory of AFC in virtual environment is predicted with high precision; When the prediction results are converted into parameters that can drive the creeping of the AFC under the virtual environment, the virtual conversion results are also of high accuracy, so the conversion results can be used as one of the criteria for determining the extent of creeping of the AFC under the virtual environment. However, there is a certain difference between the prediction results and the conversion results, which may be due to the impact of the collision of the physical engine installed on the equipment during the propulsion process, and the impact of the change of y coordinate value has not been taken into account in the established virtual conversion model.
- (3) According to the judgment of the degree of creeping of the AFC, it is found that the degree of creeping is relatively high, so it is necessary to take timely control measures. Starting from the machine head, the short knife is used to cut the coal downward, and finally the knife is used to cut through. The method of one-way frame shifting and sliding is adopted from the machine head to the tail. Feed every 20 hydraulic supports, and finally cut through the cutter from the tail to the head, so as to realize the rotary inclination adjustment of the fully mechanized working face and gradually reverse the creeping of the AFC.

6 Conclusion

Based on the Digital Twin theory and starting from the mechanism of problem occurrence, this paper takes the discrimination method of engineering problem of creeping of AFC as an example, integrates virtual reality technology with Bi-LSTM prediction algorithm, combines relevant decision-making reasoning algorithm and establishes the engineering problem prediction based on the fusion iteration of Digital Twin and prediction algorithm based on Fuzzy reasoning. The conclusions are as follows:

- (1) In this paper, a mechanism for analyzing the reasons of the creeping of AFC based on Digital Twin and grey correlation analysis is proposed. According to the reasons for the creeping of the AFC in the physical environment and mapped to the specific virtual factors in the virtual environment, a multi-factor analysis mechanism based on fuzzy grey correlation analysis method is established, which can determine the priority among the influencing factors. This is very important to the parameter configuration of the virtual environment and indirectly ensure the reliability of the final decision-making result.
- (2) The prediction method of AFC running track based on Bi-LSTM network in virtual environment is proposed. In the created virtual environment, the key operation information of equipment is extracted, and the established prediction model is used to predict the future operation information of equipment. On the premise of ensuring high prediction accuracy, the prediction results are used to provide data support for the determination of equipment operation health status.
- (3) The decision-making mechanism of the creeping of AFC based on fuzzy evidence reasoning is established. According to the prediction trajectory conversion model established in this paper, the future operation information of equipment in virtual environment is obtained. After fuzzifying the judgment degree of engineering problems with the fuzzy comprehensive evaluation method, and integrating the movement of the equipment with the D-S evidence theory, the judgment mechanism of the creeping of AFC is finally established. The judgment results can provide a reference for the operation state judgment of equipment and process adjustment in the physical environment.
- (4) The research framework proposed in this paper can provide research ideas for engineering problems in the production process of other industries. If the virtual interface is reserved in the established virtual scene, the virtual real two-way control technology is used to monitor the production scene driven by real-time data, and the deep learning prediction algorithm such as Bi-LSTM is used to predict the operation state of the equipment. The corresponding treatment measures are formulated in advance according to the established accident judgment mechanism, rehearsed in the virtual scene, and the treatment scheme is dynamically modified according to the virtual operation results. Such iterative operation until the optimal scheme is determined, and finally the health state prediction and response measures of the whole scene driven by real-time mining data are formulated in advance.

Acknowledgements This research was supported by the Central Guidance on Local Science and Technology Development Fund of Shanxi Province (YDZISX2022A014); Shanxi 1331 Project(1331); Fund Program for the Scientific Activities of Selected Returned Overseas Professionals in Shanxi Province(20230008), Research Project Supported by Shanxi Scholarship Council of China (2023-071), and the National Natural Science Foundation of China (52004174) .

Author contributions S.L. and J.X. carried out conceptual analysis; X.W. and J.X. determined the structure of the paper; X.W. and J.X. applied for fundings; S.L. wrote the main manuscript text; S.L. and J.X.

conducted literature review and investigation; S.L. and X.W. determined the specific formula; X.W. managed the whole thesis; S.L. and F.G. completed the construction of simulation environment and test platform; S.L., J.X. and F.G. conducted data processing; S.L., X.Wn. revised the article format.

Declarations

Competing interests The authors declare that they have no known competing financial interests or personal relationships that could have appeared to influence the work reported in this paper.

Open Access This article is licensed under a Creative Commons Attribution 4.0 International License, which permits use, sharing, adaptation, distribution and reproduction in any medium or format, as long as you give appropriate credit to the original author(s) and the source, provide a link to the Creative Commons licence, and indicate if changes were made. The images or other third party material in this article are included in the article's Creative Commons licence, unless indicated otherwise in a credit line to the material. If material is not included in the article's Creative Commons licence and your intended use is not permitted by statutory regulation or exceeds the permitted use, you will need to obtain permission directly from the copyright holder. To view a copy of this licence, visit <http://creativecommons.org/licenses/by/4.0/>.

References

- Bowen J, Lai R, Bahler D (1992) Fuzzy semantics and fuzzy constraint networks. In: IEEE International Conference on Fuzzy Systems. San Diego, CA, USA, pp 1009–1016. <https://doi.org/10.1109/FUZZY.1992.258793>
- Cai N, Xie J, Wang X et al (2023) Method for the relative pose reconstruction of hydraulic supports driven by digital twins. *IEEE Sens J* 23(5):P4707–4719. <https://doi.org/10.1109/JSEN.2023.3236971>
- CSIRO (2021) Creep Control. Retrieved from <http://www.lascautomation.com/dev/index.php/newoptimi-se/newcontrol/newcreepcontrol>. Accessed December 5, 2021.
- Dempster AP (1967) Upper and lower probabilities induced by a multivalued mapping. *Ann Math Stat* 38(2):325–339
- Dempster AP (1968) Generalization of Bayesian Inference. *Journal of the Royal Statistical Society. Series B* 30:205–247
- Deng J (1988) Properties of relational space for grey systems. *Grey System*. China Ocean Press, Beijing
- Feng YY, Ming SL, Bo ML (2023) Dynamic prediction of moving trajectory in pipe jacking: GRU-based deep learning framework. *Front Struct Civ Eng* 17(7):994–1010. <https://doi.org/10.1007/s11709-023-0942-5>
- Ge X, Xie J, Wang X et al (2020) A virtual adjustment method and experimental study of the support attitude of hydraulic support groups in propulsion state. *Measurement* 158:107743. <https://doi.org/10.1016/j.measurement.2020.107743>
- Guo J, Zhao N, Sun L et al (2019) Modular based flexible digital twin for factory design. *J Amb Intel Hum Comp* 10:1189–1200. <https://doi.org/10.1007/s12652-018-0953-6>
- Hochreiter S, Schmidhuber J (1997) Long short-term memory. *Neural Comput* 9(8):1735–1780. <https://doi.org/10.1162/neco.1997.9.8.1735>
- Holm M (2014) The effect of longitudinal inclination in automatic controlled shearer workfaces. In: 14th SGEM GeoConference on Science and technologies in geology, exploration and mining, Albena, Bulgaria, pp 653–663. <https://doi.org/10.5593/SGEM2014/B13/S3.085>
- Hu D (2016) Mechanical system analysis and experimental research of scraper conveyor. Dissertation, China University of Mining & Technology
- Huang Z, Wang F, Zhang S (2020) Research on the architecture and key technologies of intelligent coal mining system. *J China Coal Soc* 45:1959–1972. <https://doi.org/10.13225/j.cnki.jccs.zn20.0348>
- Jie W, Zhijie Z, Hu C et al (2021) Performance evaluation of aerospace relay based on evidential reasoning rule with distributed referential points. *Measurement* 182:109667. <https://doi.org/10.1016/j.measurement.2021.109667>
- Kang HS, Lee JY, Choi S et al (2016) Smart manufacturing: Past research, present findings, and future directions. *Int J Pr Eng Man-Gt* 3:111–128. <https://doi.org/10.1007/s40684-016-0015-5>

- Le TD, Ahn KK (2011) A vibration isolation system in low frequency excitation region using negative stiffness structure for vehicle seat. *J Sound Vib* 330:6311–6335. <https://doi.org/10.1016/j.jsv.2011.07.039>
- Li S, Xie J, Wang X et al (2022) A method of straightening armoured face conveyor based on space kinematics of reserve pushing mechanism. *Proc Inst Mech Eng C J Mech Eng Sci* 236(6):3073–3092. <https://doi.org/10.1177/09544062211036103>
- Li S, Xie J, Ren F, et al (2021) Virtual straightening of scraper conveyor based on the position and attitude solution of industrial robot model. *Int J Coal Sci Techn* 8:1149–1170. <https://doi.org/10.1007/s40789-020-00389-y>
- Michael S, Hainsworth D (2005) Outcomes of the landmark long-wall automation project with reference to ground control issues. In: *The 24th International Conference on Ground Control in Mining*. Lakewood Scanticon Resort&Conference Center, Morgantown, WV, USA, pp 1–8. <http://hdl.handle.net/102.100.100/183258>
- Min K, Kim D, Park J et al (2019) RNN-Based Path Prediction of Obstacle Vehicles With Deep Ensemble. *IEEE T Veh Technol* 68(10):10252–10256. <https://doi.org/10.1109/TVT.2019.2933232>
- Niu JF (2015) Automatic incline adjustment and anti-skid control system development for full-mechanized mining face. *Coal Min Techno* 20(2):32–34. <https://doi.org/10.13532/j.cnki.cn11-3677/d.2015.02.010>
- Özer İ, Efe SB, Özbay H (2021) CNN/Bi-LSTM-based deep learning algorithm for classification of power quality disturbances by using spectrogram images. *Int Trans Electr Energy Syst* 31(12):13204. <https://doi.org/10.1002/2050-7038.13204>
- Peng SS, Du F, Cheng J et al (2019) Automation in U.S. longwall coal mining: A state-of-the-art review. *Int J Min Sci Technol* 29:151–159. <https://doi.org/10.1016/j.ijmst.2019.01.005>
- Qiang L (2020) Study on Architecture of Intelligent Manufacturing Theory. *Chin J Mech Eng-En* 31:24–36. <https://doi.org/10.3969/j.issn.1004-132X.2020.01.004>
- Quan R, Zhu L, Wu Y (2021) Holistic LSTM for Pedestrian Trajectory Prediction. *IEEE T Image Process* 30:3229–3239. <https://doi.org/10.1109/TIP.2021.3058599>
- Shafer G (1976) *A Mathematical Theory of Evidence*. Princeton University Press, Princeton
- Shen H, Xie J, Li J et al (2021) Collision Detection of Virtual Powered Support Groups Under Complex Floors. *IEEE T Instrum Meas* 70:1–13. <https://doi.org/10.1109/TIM.2021.3104412>
- Shenguang H, Xing X, Ju X et al (2023) Adaptive control of dual-motor autonomous steering system for intelligent vehicles via Bi-LSTM and fuzzy methods. *Control Eng Pract* 130:105362. <https://doi.org/10.1016/j.conengprac.2022.105362>
- Simone Z, Kefato ZT, Sarunas G et al (2022) Pedestrian trajectory prediction with convolutional neural networks. *Pattern Recogn* 121:108252. <https://doi.org/10.1016/j.patcog.2021.108252>
- Song X, Wang L (2014) Research on Mining Engineering with Dual Gradient High Inclination-Angle Fully Mechanized Mining Technology. *Adv Mat Res* 977:231–234. <https://doi.org/10.4028/www.scientific.net/AMR.977.231>
- Tong Y, Wu P, He J et al (2021) Bearing Fault Diagnosis Via Combining Deep Residual Shrinkage Network and Bidirectional LSTM. *Meas Sci Technol* 33(3):034001. <https://doi.org/10.1088/1361-6501/ac37eb>
- Verma P (2013) An experimental investigation of the creep behavior of an underground coalmine roof with shaEle formation. West Virginia University, Department of Mining Engineering, Morgantown
- Wang J, Huang Z (2017) The Recent Technological Development of Intelligent Mining in China. *Eng* 3(4):439–444. <https://doi.org/10.1016/J.ENG.2017.04.003>
- Wang S, Wang S, Liu W (2020) Longwall Retreat and Creep Measurement Based on UWB Radar Imaging Method. *Math Probl Eng* 2(2020):1–13. <https://doi.org/10.1155/2020/4056246>
- Wang Q, Cai M, Wei G (2022) A scenario analysis under epistemic uncertainty in Natech accidents: imprecise probability reasoning in Bayesian Network. *Environ Res Commun* 4(1):015008. <https://doi.org/10.1088/2515-7620/ac47d4>
- Xie J, Li S, Wang X (2022) A digital smart product service system and a case study of the mining industry: MSPSS. *Adv Eng Inform* 53:101694. <https://doi.org/10.1016/j.cie.2022.108050>
- Xiping W, Hongyu Y, Hu C et al (2022) Long-term 4D trajectory prediction using generative adversarial networks. *Transport Res C-Emer* 136:103554. <https://doi.org/10.1016/j.trc.2022.103554>
- Xu YQ (1999) *Coal Ming*. China University of Mining and Technology Press, BeiJing
- Yager RR (1987) On the dempster-shafer framework and new combination rules. *Inform Sci* 41(2):93–137. [https://doi.org/10.1016/0020-0255\(87\)90007-7](https://doi.org/10.1016/0020-0255(87)90007-7)
- Yeming D, Qiong Z, Mingming L et al (2022) Improving the Bi-LSTM model with XGBoost and attention mechanism: A combined approach for short-term power load prediction. *Appl Soft Comput* 130:109632. <https://doi.org/10.1016/j.asoc.2022.109632>
- Zhang KX, Li SB, He MC et al (2018) Study on key technologies of intelligent unmanned coal mining series: study on diagonal adjustment control technology of intelligent fully-mechanized coal mining face. *Coal Sci Techno* 46:139–149. <https://doi.org/10.13199/j.cnki.cst.2018.01.020>

Publisher's Note Springer Nature remains neutral with regard to jurisdictional claims in published maps and institutional affiliations.